

January 23, 2018

## Retraction Notice

Retraction: Zhang J, Xia X, Li S, Ran W. (2018) Response of methane production via propionate oxidation to carboxylated multiwalled carbon nanotubes in paddy soil enrichments. PeerJ 6:e4267 [10.7717/peerj.4267](https://doi.org/10.7717/peerj.4267)

Immediately after publication, readers alerted the authors that the nanotubes used in their experiments may not have possessed the electrical conductivity that the authors had assumed (based on the manufacturer's data). The authors tested the nanotubes in question, and confirmed that their electrical conductivity is too low to be able to rely on their results. As a result, the conclusions in the article cannot be relied upon, and all the authors have agreed to retract this article. The authors would like to thank the readers who alerted them to this issue.

This Retraction updates an Expression of Concern which was issued on January 18th 2018.

PeerJ Editorial Office. 2018. Retraction: Response of methane production via propionate oxidation to carboxylated multiwalled carbon nanotubes in paddy soil enrichments. PeerJ 6:e4267/retraction  
<https://doi.org/10.7717/peerj.4267/retraction>



# Response of methane production via propionate oxidation to carboxylated multiwalled carbon nanotubes in paddy soil enrichments

Jianchao Zhang<sup>1</sup>, Xingxuan Xia<sup>2</sup>, Siliang Li<sup>1</sup> and Wei Ran<sup>3</sup>

<sup>1</sup>Institute of Surface-Earth System Science, Tianjin University, Tianjin, China

<sup>2</sup>College of Urban and Environmental Sciences, Peking University, Beijing, China

<sup>3</sup>Jiangsu Provincial Coordinated Research Center for Organic Solid Waste Utilization, Nanjing Agricultural University, Nanjing, China

## ABSTRACT

Carboxylated multiwalled carbon nanotubes (MWCNTs-COOH) have become a growing concern in terms of their fate and toxicity in aqueous environments. Methane (CH<sub>4</sub>) is a major product of organic matter degradation in waterlogged environments. In this study, we determined the effect of MWCNTs-COOH on the production of CH<sub>4</sub> from propionate oxidation in paddy soil enrichments. The results showed that the methanogenesis from propionate degradation was accelerated in the presence of MWCNTs-COOH. In addition, the rates of CH<sub>4</sub> production and propionate degradation increased with increasing concentrations of MWCNTs-COOH. Scanning electron microscopy (SEM) observations showed that the cells were intact and maintained their structure in the presence of MWCNTs-COOH. In addition, SEM and fluorescence in situ hybridization (FISH) images revealed that the cells were in direct contact with the MWCNTs and formed cell-MWCNTs aggregates that contained both bacteria and archaea. On the other hand, nontoxic magnetite nanoparticles (Fe<sub>3</sub>O<sub>4</sub>) had similar effects on the CH<sub>4</sub> production and cell integrity as the MWCNTs-COOH. Compared with no nanomaterial addition, the relative abundances of *Geobacter* and *Methanosarcina* species increased in the presence of MWCNTs-COOH. This study suggests that MWCNTs-COOH exerted positive rather than cytotoxic effects on the syntrophic oxidation of propionate in paddy soil enrichments and affected the bacterial and archaeal community structure at the test concentrations. These findings provide novel insight into the consequences of nanomaterial release into anoxic natural environments.

Submitted 24 October 2017  
Accepted 25 December 2017  
Published 12 January 2018

Corresponding author  
Wei Ran, ranwei@njau.edu.cn

Academic editor  
Junkuo Gao

Additional Information and  
Declarations can be found on  
page 12

DOI 10.7717/peerj.4267

© Copyright  
2018 Zhang et al.

Distributed under  
Creative Commons CC-BY 4.0

OPEN ACCESS

**Subjects** Environmental Sciences, Microbiology, Soil Science, Ecotoxicology, Environmental Impacts

**Keywords** Carboxylated, MWCNTs, Syntrophic methanogenesis, Propionate, Anaerobic, Paddy soil enrichment

## INTRODUCTION

Carbon nanotubes (CNTs) are hollow cylinders with microscale lengths and nanoscale diameters that are composed of aligned benzene rings (Iijima, 1991). Multi-walled carbon nanotubes (MWCNTs) are widely used due to their unique antimicrobial properties

and physicochemical properties including high electrical conductivity, as well as their superior chemical and mechanical stability (*De Volder et al., 2013*). As a consequence of the rapid increase in the commercial-scale application of MWCNTs, they will accidentally or inevitably enter various environments (*Petersen et al., 2011*). Release of CNTs could occur at all steps in the life cycle of consumer products. In addition, relevant release scenarios of CNTs are described in detail: injection molding, manufacturing, sports equipment, fuel system components, landfills, windmill blades, electronics, tires, textiles, and incineration (*Nowack et al., 2013*). Release of CNTs from products can potentially occur by two pathways: (a) where free CNTs are released directly, or (b) where release of particles with CNTs embedded in the matrix (*Nowack et al., 2013*). For instance, CNTs fate models predict that the CNTs concentrations are between 6.6 ng/L and 18 ng/L in the plant effluent and with a modeled increase in sediment deposition rate of 40 ng/kg to 229 ng/kg per year in United States (*Gottschalk et al., 2009*).

Biogenic methane ( $\text{CH}_4$ ) production is carried out by oxygen sensitive methanogenic archaea and hence is restricted to anoxic environments, such as freshwater sediments and rice field soils (*Mach et al., 2015*). Paddy soil is one of the important natural  $\text{CH}_4$  sources (*Conrad, 2009*). It is known that interspecies electron exchange is involved in the decomposition of complex organic substances and  $\text{CH}_4$  production in anoxic environments with  $\text{H}_2$  or formate serving as electron carriers (*Stams & Plugge, 2009*). Recently, direct interspecies electron transfer (DIET) has been proposed as a novel alternative to interspecies electron transfer in methanogenesis (*Rotaru et al., 2014a*). DIET has been described as cell–cell extracellular electron transfer via electric currents through biological structures (i.e., microbial pili) or abiological conductive solid materials, such as magnetite ( $\text{Fe}_3\text{O}_4$ ), granular activated carbon and biochar (*Liu et al., 2015; Shrestha & Rotaru, 2014*). In particular,  $\text{Fe}_3\text{O}_4$ , a common iron mineral in soils and sediments, represents a natural material that can accelerate syntrophic  $\text{CH}_4$  production in paddy soil and anaerobic sludge digesters (*Kato, Hashimoto & Watanabe, 2012; Li et al., 2015; Liu et al., 2015; Viggli et al., 2014*).

Unlike  $\text{Fe}_3\text{O}_4$ , granular activated carbon and biochar, MWCNTs have been shown to inhibit the growth and activity of a range of microorganisms in pure culture and exposure to mixed microbial community, including bacteria and protozoa (*Kang, Mauter & Elimelech, 2008; Zhao & Liu, 2012*). Recent research by *Salvador et al. (2017)* demonstrated that conductive MWCNTs could accelerate methanogenesis not only by facilitating DIET in the co-cultures from environmental enrichments (*Zhang & Lu, 2016*) but also in pure cultures of methanogens provided with typical methanogenic substrates. However, it is still unknown how and why methanogenesis gets stimulated by MWCNTs. Furthermore, MWCNTs can potentially be released into the aquatic ecosystem via wastewater discharge and runoff from areas around waste dumps and manufacturing plants, eventually accumulating in the paddy soils or sediments (*Farré et al., 2009; Nowack et al., 2013; Petersen et al., 2011*). Paddy soil is the most typical and widespread agricultural soil in Asia. In addition, paddy soil represents a hotspot of the  $\text{CH}_4$  emission and production, because the flooded conditions during rice growth (*Conrad, 2009*). Some studies had shown that MWCNTs had positive effect on the methanogenesis from anaerobic digesters

(Ambuchi *et al.*, 2017) and lake sediment (Zhang & Lu, 2016), but the effect of MWCNTs on a methanogenic community from paddy soil has not been previously shown. Propionate is one of the major intermediates in the methanogenic degradation of complex organic matter in paddy soil (Gan *et al.*, 2012). In the present study, to address the possible influence of carboxylate-functionalized MWCNTs (MWCNTs-COOH) on syntrophic methanogenesis from propionate oxidation, methanogenic communities were enriched from paddy soil in the presence and absence of MWCNTs-COOH. Fluorescence *in situ* hybridization (FISH) and scanning electron microscopy (SEM) were used to visualize the interactions between microbial cells and MWCNTs-COOH. The effect of MWCNTs-COOH on the microbial consortia was also investigated. The results of this study will provide useful information to understand the response of methanogenic communities to MWCNTs-COOH in paddy soil.

## MATERIALS AND METHODS

### Nanomaterial preparation and characterization

Commercially available carboxylic (-COOH) functionalized MWCNTs were purchased from DK Nano Technology Co. (Beijing, China). According to the manufacturer, the purity was more than 99% by mass, the average diameter and length of MWCNTs-COOH were approximately 10–20 nm and 10–30  $\mu\text{m}$ , and the COOH content was approximately 2% (w/w). A ten percent (w/v) MWCNTs-COOH stock water suspension was used for the experiments. Nano-sized  $\text{Fe}_3\text{O}_4$  particles (50–100 nm) were purchased from Sigma-Aldrich (637106; St. Louis, MO, USA).

### Inoculum source and anaerobic media

Flooded paddy soil was collected from Tianjin, northern China (43°44'N 126°30'E). The soil had the following characteristics: total organic carbon content of 1.90%, total nitrogen content of 0.12% and pH ( $\text{H}_2\text{O}$ ) 7.85. The soil is classified as a clay texture. The soil samples were collected in July 2016 at a depth of 0–20 cm. Twelve soil cores (approximately 5 cm in diameter) were taken from the flooded paddy field and mixed to form one composite sample. Soil samples were placed in sealed bottles that were filled and transported to the lab as soon as possible. The soil samples were stored at 4 °C until use.

HEPES-buffered (30 mM, pH 7) anaerobic basal medium was used for enrichment and subsequent transfers. The basal medium preparation followed a previously described protocol (Lü & Lu, 2012). Sodium propionate was added as a substrate at a final concentration of 10 mM through injection via an aseptic syringe into the bottled culture medium. A concentration of up to 10 mM propionate can be locally found during the anaerobic decomposition of organic matter (Gan *et al.*, 2012).

### Enrichment procedures

For the initial enrichment (first enrichments), approximately 5 g of fresh soil (2.13 g dry soil) was transferred in triplicate into sterile 120 ml serum bottles filled with 40 ml of medium and closed with butyl rubber stoppers. Four treatments were conducted in the enrichments, including a no nanomaterial supplementation control treatment (CK-1),

MWCNTs-COOH supplementation treatment 1 (MWCNTs-COOH-1, final concentration of 1 g/L), MWCNTs-COOH treatment 2 (MWCNTs-COOH-2, final concentration of 0.1 g/L) and nanoFe<sub>3</sub>O<sub>4</sub> supplementation treatment (the final concentration of 10 mM as Fe atom). The addition of electrically conductive Fe<sub>3</sub>O<sub>4</sub> nanoparticles (natural occurring mineral in environments) was used as positive control for evaluating the effects from MWCNTs-COOH.

When the CH<sub>4</sub> production from the MWCNTs-COOH treatment 1 approached a plateau, a portion of the culture from the MWCNTs-COOH treatment 1 was transferred to a bottle containing 40 ml of fresh medium (next enrichment culture) (Figure S1). For all the transfers in this study, the inoculum size was 4% (v/v). Four treatments with inocula from MWCNTs-COOH-1 were performed for the subsequent enrichments. The first and fourth transfers are only shown in the present study because the first to fourth enrichments behaved similarly. In addition, another batch of enrichments (CK-2) was conducted simultaneously with inocula from the no nanomaterial supplementation treatment (Figure S1). The schematic diagram of the experimental design is shown in Fig. 1. All the enrichments were incubated statically in the dark at 30 °C under an atmosphere of N<sub>2</sub>/CO<sub>2</sub> [80:20 (V/V)].

### Chemical analyses

The CH<sub>4</sub> concentration was analysed using a gas chromatograph (7890; Agilent Technologies, Santa Clara, CA, USA) equipped with flame ionization detector (FID) (Peng *et al.*, 2008). Gas samples (100 µl) were collected from the headspace using a Pressure-Lok precision analytical syringe (Bation Rouge, LA USA) every two to five days. Liquid samples (0.5 ml) were collected every four to nine days with a sterile syringe, centrifuged, and filtered through 0.22 µm filters (Millipore, Burlington, MA, USA). The concentrations of propionate were analysed by high-pressure liquid chromatography (HPLC) with a Zorbax SB-AQ C18 column (Agilent Technologies, Santa Clara, CA, USA) (Krumböck & Conrad, 1991).

### Microscopy analysis

The cultures in the fourth enrichments were subjected to microscopy when the cell communities were enriched. The cells in the CK-1, Fe<sub>3</sub>O<sub>4</sub> and MWCNTs-1 treatments were collected using a sterile syringe, fixed with 2.5% (wt/vol) glutaraldehyde in phosphate-buffered saline, and sequentially dehydrated with serial ethanol dilutions (20, 40, 60, 80, 95 and 100% (v/v) with every 10 min per step). The dried samples were coated with platinum and imaged using scanning electron microscopy (FEI NanoSEM 430).

In addition, fluorescence *in situ* hybridization (FISH) analysis was performed on 4% paraformaldehyde-fixed samples according to a procedure described previously (Moter & Göbel, 2000). Oligonucleotide probes specific for bacteria (Cy3-labeled EUB338mix probes) and archaea (FITC-labeled ARC915 probe) were used in this study. The details of the probes used are available in probeBase (<http://probebase.csb.univie.ac.at/>) (Greuter *et al.*, 2016). The labelled samples were visualized using epifluorescence microscopy (Axio Imager D2; ZEISS, Oberkochen, Germany).

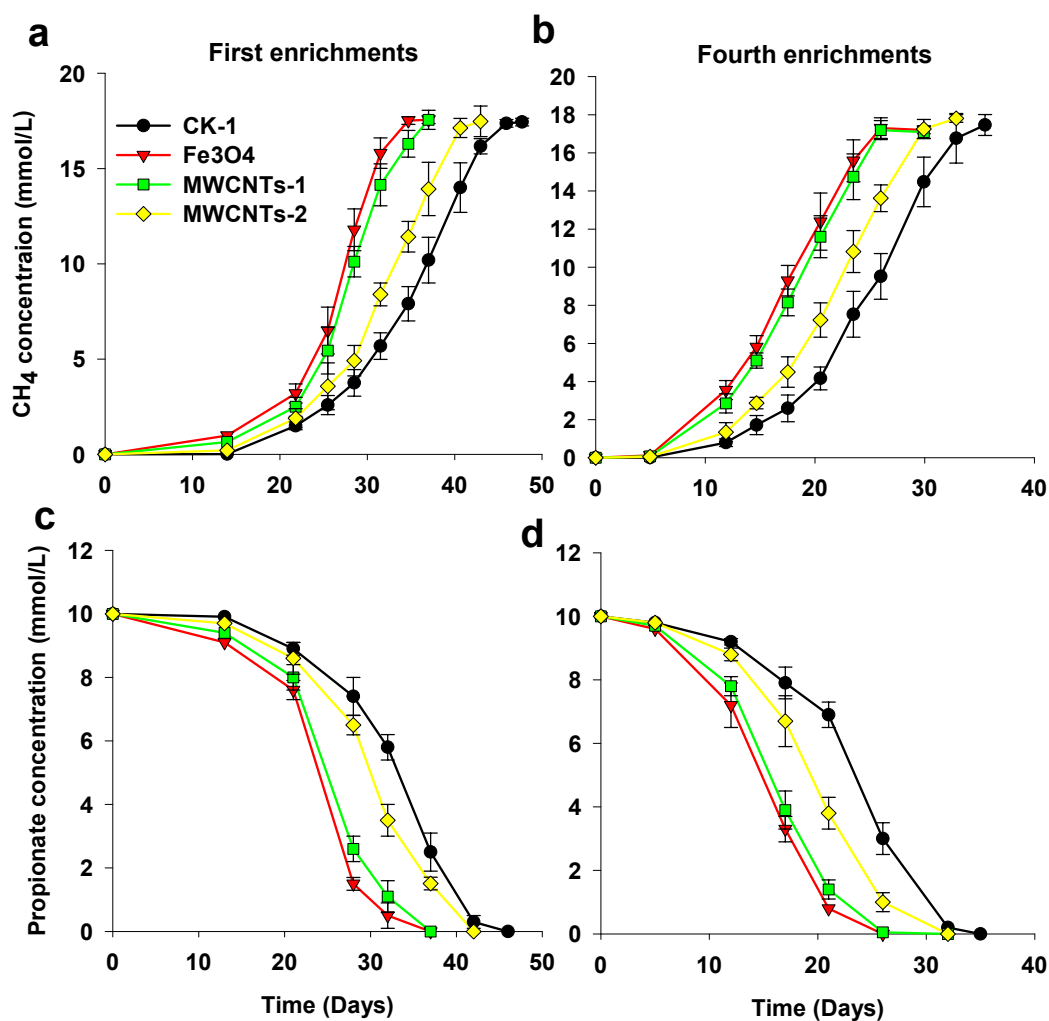


**Figure 1** Effects of MWCNTs-COOH and Fe<sub>3</sub>O<sub>4</sub> supplementation on the production of CH<sub>4</sub> (A, B) and the degradation of propionate (C, D) for the first and fourth enrichments. Error bars represent the standard deviation of three replicates. MWCNTs-1: MWCNTs-COOH supplementation treatment 1 with a final concentration of 1 g/L; MWCNTs-2: MWCNTs-COOH supplementation treatment 2 with a final concentration of 0.1 g/L.

Full-size DOI: [10.7717/peerj.4267/fig-1](https://doi.org/10.7717/peerj.4267/fig-1)

### Molecular analysis of the microbial community

The cells in the MWCNTs-COOH-1 and CK-2 treatments were harvested from triplicate cultures at the fourth enrichments. In addition, the cells from different treatments were collected in the mid-log phase (CH<sub>4</sub> concentration about 12 mM) by syringe. Total DNA was extracted using the FastDNA SPIN Kit (MP Biomedicals, Santa Ana, CA, USA) according to the manufacturer's protocol. Prior to DNA extraction, sonication was performed to separate the microbial cells from the MWCNTs. The DNA was extracted from each replicate and stored at  $-20^{\circ}\text{C}$ .

We used high throughput Miseq sequencing for the analysis of the microbial community in the enriched cultures. The V3–V4 universal primers 314F/805R were used to determine

the bacterial communities. In addition, the 349F/806R primers were used to amplify the archaeal 16S rRNA genes. Sequencing was performed using the Illumina Miseq 2 × 300 bp platform (San Diego, CA, USA) by Sangon Biotech Company (Shanghai, China).

We used the Quantitative Insights Into Microbial Ecology (QIIME) ([Caporaso et al., 2010](#)) and UPARSE pipeline ([Edgar, 2013](#)) to treat the raw sequencing data. Barcodes and standard primer sets were excluded. The UPARSE pipeline was used to select the operational taxonomic units (OTUs), and the sequences were assigned to OTUs with 97% similarity. Then, a representative OTU sequence was assigned to a taxonomic identity using RDP classifier (<http://rdp.cme.msu.edu>) ([Wang et al., 2007](#)) with a default confidence threshold of 0.8–1.0. Raw sequencing reads have been deposited into the NCBI SRA with the accession number [SRP108450](#).

## RESULTS

### Effects of MWCNTs-COOH on CH<sub>4</sub> production

The effect of MWCNTs-COOH on CH<sub>4</sub> production by methanogenic enrichment cultures was assessed ([Fig. 1](#)). Two enrichments (first and fourth) were revealed in the present study because the first to fourth enrichments behaved similarly. In the incubations, the results showed that the addition of Fe<sub>3</sub>O<sub>4</sub> and MWCNTs-COOH increased the rate of methane production from propionate oxidation. In addition, CH<sub>4</sub> production at a MWCNTs-COOH concentration of 1 g/L was faster than that at 0.1 g/L ([Figs. 2A, 2B](#)). In the first enrichments ([Fig. 1A](#)), the time preceding the completion of CH<sub>4</sub> production was much shorter in the assays with Fe<sub>3</sub>O<sub>4</sub> and with high concentration of MWCNTs-COOH (approximately 31 days) than in the assays without nanomaterials (approximately 46 days) or with low concentration of MWCNTs-COOH (approximately 42 days). The production of CH<sub>4</sub> in the fourth enrichment cultures was faster than the first enrichments for all the treatments, but the stimulating effect of MWCNTs and Fe<sub>3</sub>O<sub>4</sub> remained evident.

Similarly, propionate conversion to CH<sub>4</sub> was also enhanced by the presence of Fe<sub>3</sub>O<sub>4</sub> and MWCNTs ([Figs. 1C, 1D](#)). In the first enrichment cultures, propionate degradation in the assays with Fe<sub>3</sub>O<sub>4</sub> and high concentration of MWCNTs-COOH started after a shorter lag phase and proceeded to completion more rapidly compared to the assays without nanomaterials or with low concentration of MWCNTs-COOH (36 days vs 42 or 46 days). Subsequent enrichments showed similar trends to those in the first enrichments.

In the incubations, approximately 17.8 mM CH<sub>4</sub> was produced from 10.1 mM propionate ([Fig. 1](#)). This result suggests that the syntrophic interaction in the enrichments followed the stoichiometry of the complete conversion of propionate to CH<sub>4</sub> ( $4\text{CH}_3\text{CH}_2\text{COO}^- + 4\text{H}^+ + 2\text{H}_2\text{O} \rightarrow 7\text{CH}_4 + 5\text{CO}_2$ ).

### FISH assays

The FISH images exhibited strong fluorescence bacterial (in red) and archaeal (in green) signatures in the enrichments, indicating that the cells in the MWCNTs-COOH treatment were active and intact as in the CK-1 and Fe<sub>3</sub>O<sub>4</sub> treatments ([Fig. 2](#)). Classical *Sarcina*-like shapes were dominant with filamentous cells accounting for a small fraction in the archaeal cells ([Fig. 2](#)). In addition, we found that numerous aggregates were formed irrespective of



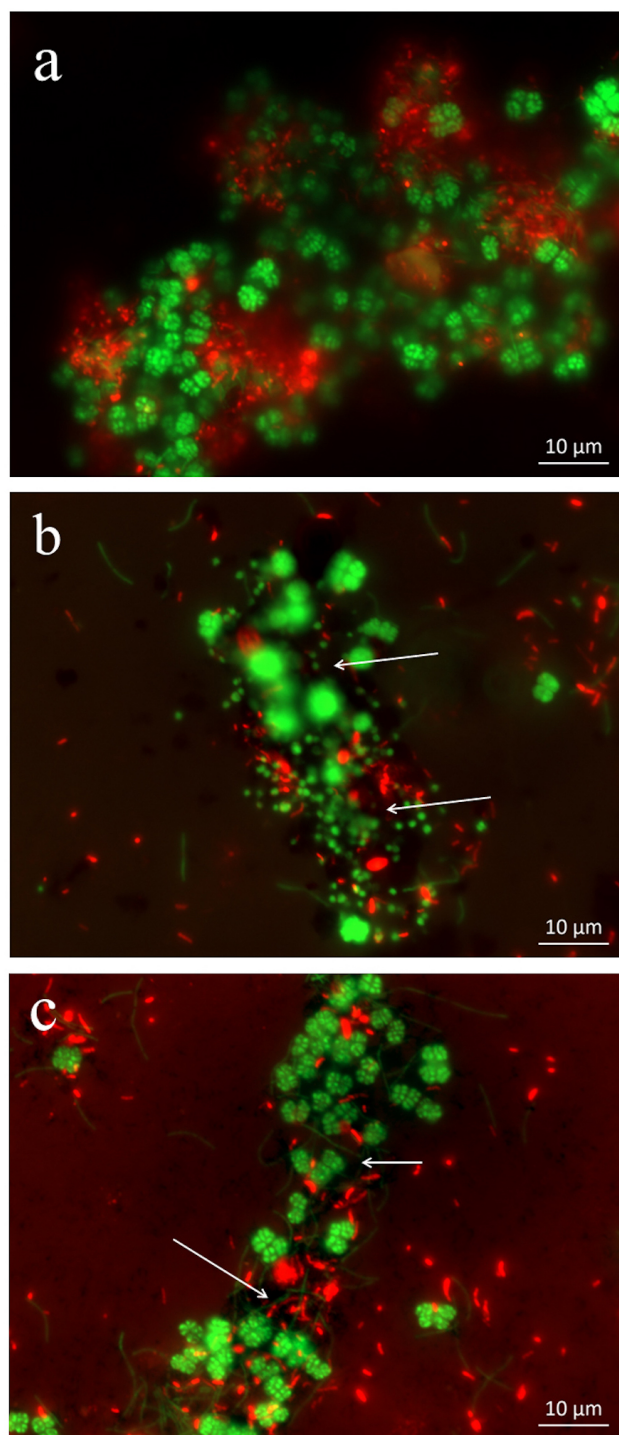


**Figure 2** Spatial distribution of archaeal (Arc915-FITC, green) and bacterial (EUB338mix-Cy3, red) cells identified by FISH in enrichments with CK-1 (A),  $\text{Fe}_3\text{O}_4$  (B) and MWCNTs-1 (C) treatments. Cell aggregates were formed irrespective of the treatment. Blurry black plots with red or dark backgrounds within the cell aggregates (indicated by white arrows) could be found in the presence of  $\text{Fe}_3\text{O}_4$  and MWCNTs-COOH.

Full-size  DOI: [10.7717/peerj.4267/fig-2](https://doi.org/10.7717/peerj.4267/fig-2)



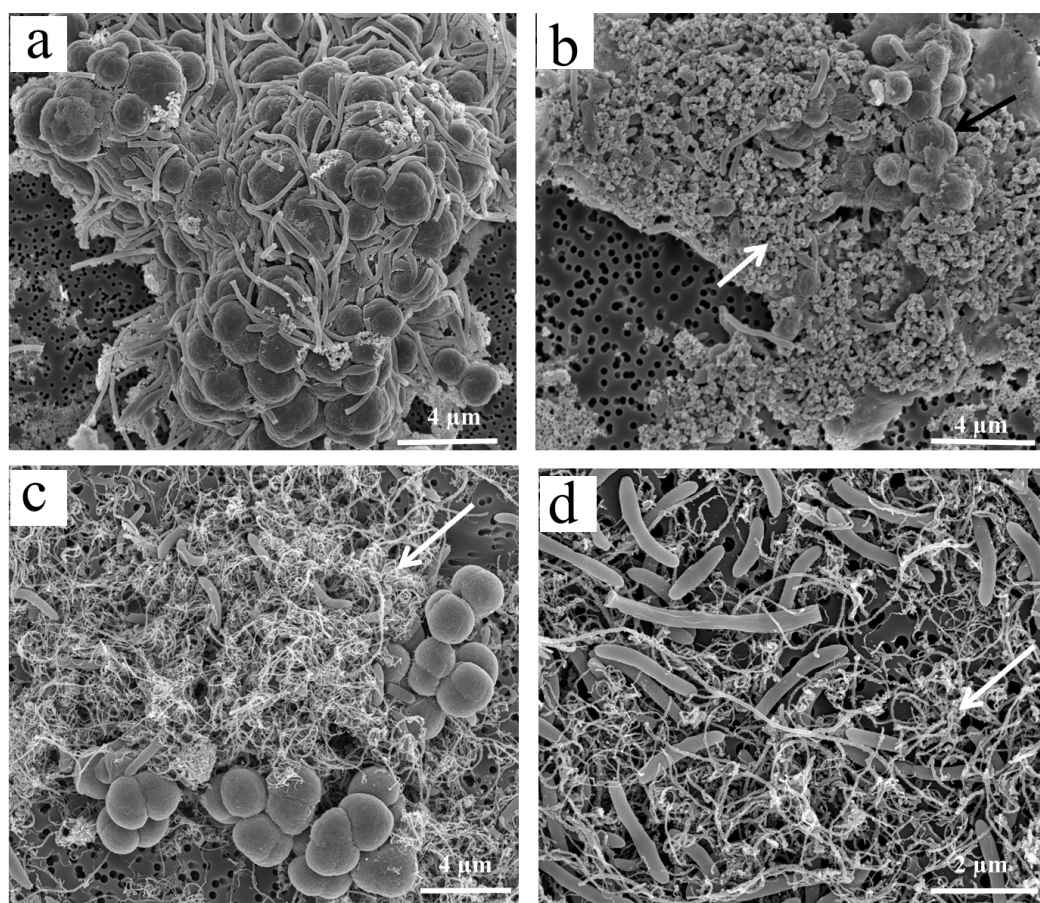


**Figure 3** Interactions between microbial cells and nanomaterials (MWCNTs-COOH and  $\text{Fe}_3\text{O}_4$ ) in the enrichment treatments by scanning electron micrographs (SEM). CK-1: (A);  $\text{Fe}_3\text{O}_4$ : (B); MWCNTs-1: (C, D). White arrows (B, C and D) indicate  $\text{Fe}_3\text{O}_4$  nanoparticles or MWCNTs-COOH.

Full-size DOI: [10.7717/peerj.4267/fig-3](https://doi.org/10.7717/peerj.4267/fig-3)

the treatment. FISH observations revealed that the bacteria were in close contact with the archaeal cells in the aggregates.

### SEM observations

Abundant aggregates were also observed by SEM (Fig. 3). In addition to short-rod and long slender-rod cells, the *Sarcina*-like cells were dominant. The bacterial and archaeal cells in the control were in close contact forming dense microbial aggregates (Fig. 3A). In the MWCNTs-COOH-1 treatment, however, most of the cells were in association with MWCNTs-COOH and formed cells-nanomaterial mixtures (Figs. 3C, 3D). Though microbial cells appeared more separated in MWCNTs-COOH compared with those with close physical proximity in the control, most of the microbial cells were interconnected by the MWCNTs-COOH. SEM observations of the enrichments where MWCNTs-COOH was replaced with nano $\text{Fe}_3\text{O}_4$ , which had similar architecture to the microbe-nanomaterial hybrid aggregates (Fig. 3B).

In addition, the SEM images showed that the cells in the MWCNTs-COOH treatment were intact and maintained their structure, similar to the cells in the control and nanoFe<sub>3</sub>O<sub>4</sub> treatments. These results indicated that no obvious cellular damage occurred when the cells were in contact with high concentration (1 g/L) of MWCNTs-COOH.

### Microbial community compositions

Analysis of the microbial communities was carried out for the fourth enrichments with the MWCNTs-COOH-1 and CK-2 treatments. In the MWCNTs-COOH-1 enrichment, the 16S rRNA gene sequencing revealed that the bacterial populations were dominated by *Smithella* (24%) and *Syntrophomonas* (19%), followed by *Geobacter* (14%), *Syntrophobacter* (9%), *Clostridium* (6%), *Pelotomaculum* (7%), *Desulfobulbus* (3.7%) and *Sulfurospirillum* (3.1%) (Fig. 4A). The archaeal community (Fig. 4B) in the MWCNTs-COOH-1 enrichment consisted mainly of *Methanosarcina* (44%) and *Methanoregula* (16%), with a minor proportion of *Methanosaeta* (12%), *Methanocella* (4%), *Methanomicrobium* (5%) and *Methanobacterium* (4%). By comparison, the predominant bacterial components in the CK-2 enrichment (Fig. 4A) consisted of *Syntrophobacter* (23%), *Pelotomaculum* (18%) *Smithella* (19%) and *Syntrophomonas* (11%) with a minor proportion of *Clostridium* (3%) and *Geobacter* (4%). In addition, the archaeal community in the CK-2 enrichment consisted of *Methanosarcina* (27%), *Methanoregula* (11%) *Methanosaeta* (8%), *Methanocella* (18%), *Methanomicrobium* (9%), *Methanobacterium* (15%).

## DISCUSSION

### MWCNTs-COOH and the cell damages

MWCNTs have been reported to cause different inhibitory effects on microorganisms (Kang, Mauter & Elimelech, 2008; Yadav, Mungray & Mungray, 2016). Previous SEM studies showed that CNT-treated cells lost their cellular integrity (flattened or misshapen) (Kang, Mauter & Elimelech, 2008). The antimicrobial mechanism probably involves oxidative stress and cell membrane damage (Du et al., 2013). Additionally, the results from Kang et al. (2007) suggested that physical interaction of CNTs with bacterial cells, rather than oxidative stress, is the primary killing mechanism. Otherwise, the antimicrobial activity of CNTs was regulated by their concentration (Das et al., 2014). In the current study, relatively high concentration of MWCNTs-COOH (1 g/L) was applied compared to previous studies on the inhibitory effects (Nouara et al., 2013; Wang et al., 2014). If the inhibitory mechanisms worked, more severe effects would be anticipated in the present experiment. However, we did not observe adverse effects in this study. Instead, the effects of MWCNTs-COOH on CH<sub>4</sub> production from propionate degradation were positive in our enrichments, similar to the effects of Fe<sub>3</sub>O<sub>4</sub>. Furthermore, the acceleration of CH<sub>4</sub> production was higher with the highest MWCNTs concentration tested (Fig. 1). FISH observations suggested that the bacterial and archaeal cells were aggregated irrespective of the treatment (Fig. 2). SEM images further verified the formation of cell-MWCNTs aggregates in the MWCNTs treatment and showed that the cells were in direct contact with the MWCNTs (Fig. 3). According to our SEM observations, penetration into the cell membranes or adverse effects on the cellular integrity did not occur.

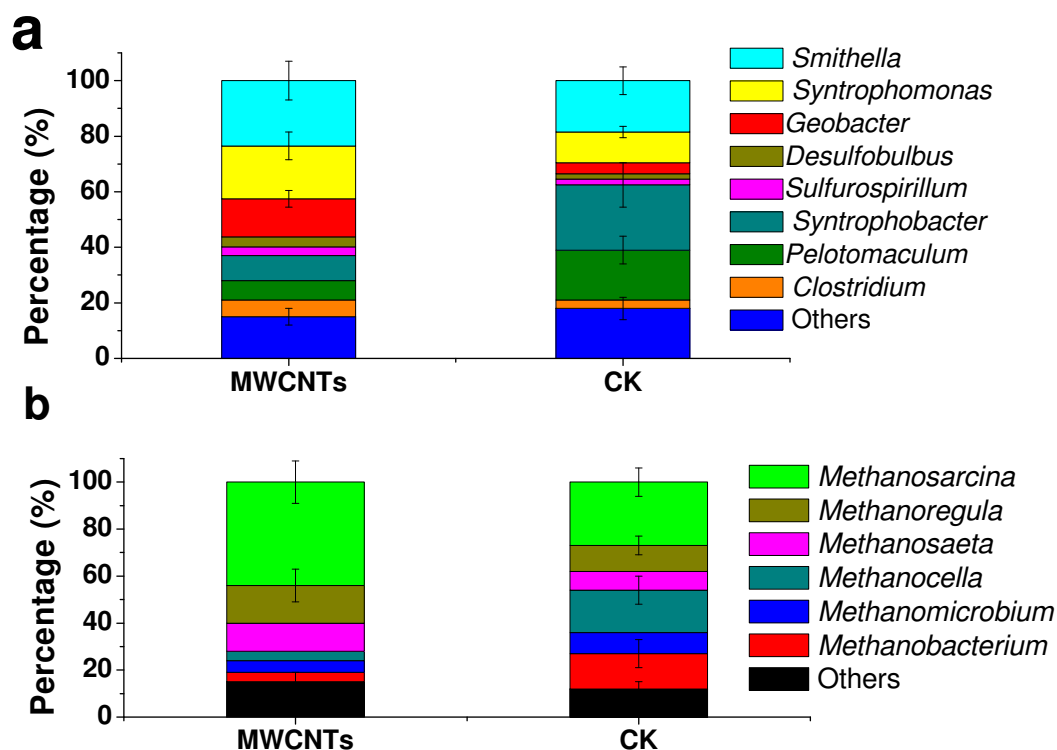


**Figure 4** The phylogenetic classification and relative abundance of the bacteria (A) and archaea (B) at the genus level in the enrichments of the MWCNTs-1 and CK-2 treatments. “Other” indicates the genus of the bacteria (A) or archaea (B) with a low relative abundance (less than 2%). The error bars represent standard deviations from the triplicate samples of each treatment.

Full-size DOI: 10.7717/peerj.4267/fig-4

The lack of inhibitory effect in the present experiment was probably due to the anaerobic conditions. Oxidative stress by MWCNTs resulted from the production of reactive oxygen species (ROS) due to the small size and high reactivity of MWCNTs (Du *et al.*, 2013). It was also shown that the MWCNTs-COOH could generate notable amounts of ROS during UVA irradiation at an intensity similar to that in the sunlight (Qu, Alvarez & Li, 2013). However, the enrichment cultivation in the present experiment was carried out in the dark and under anaerobic conditions. Thus, oxidative stress should not be a significant factor in this study. In addition, the cytotoxicity of CNTs is often attributed to the physicochemical properties of CNTs. The carboxylate functionalization of MWCNTs is thought to make the nanomaterials more biocompatible than the pristine MWCNTs due to their improved hydrophilicity and dispersion in the biological media (Vardharajula *et al.*, 2012). The CNTs used in this study are carboxylated MWCNTs.

### MWCNTs-COOH and microbial community in the syntrophic consortia

Instead of inhibition, the addition of MWCNTs-COOH substantially facilitated the syntrophic production of CH<sub>4</sub> from propionate oxidation. Stimulation of CH<sub>4</sub> production in the presence of Fe<sub>3</sub>O<sub>4</sub> has been reported previously (Kato, Hashimoto & Watanabe, 2012;

*Li et al., 2015; Liu et al., 2015; Rotaru et al., 2014a; Viggi et al., 2014; Zhang & Lu, 2016*). All the existing reports suggested the  $\text{Fe}_3\text{O}_4$  acts as a conductor that facilitates or accelerates the transfer of electrons between *Geobacter* and acetotrophic methanogens (*Methanosarcina* and *Methanosaeta*). *Geobacter* species are widespread in anoxic soils and typically carry out a dissimilatory reduction on extracellular electron acceptors, such as Fe(III), coupled with the oxidation of acetate and other electron donors (*Mahadevan, Palsson & Lovley, 2011; Richter, Schicklberger & Gescher, 2012*). Previous studies have demonstrated that *Geobacter* could participate in the syntrophic oxidation of propionate in the paddy soil under methanogenic conditions by stable-isotope probing (*Gan et al., 2012; Lueders, Pommerenke & Friedrich, 2004*). The microbial mechanisms of DIET between *Geobacter* and methanogens were extensively studied (*Holmes et al., 2017; Liu et al., 2012; Morita et al., 2011; Rotaru et al., 2014a; Rotaru et al., 2014b*). Electrical connections that support the DIET capacity of *Geobacter* include electrically conductive pili (e-pili) and cytochromes. The presence of *Geobacter* species is often equated with the occurrence and capacity for DIET (*Holmes et al., 2017*). Compared with CK-2, the relative abundance of *Geobacter* was increased in the presence of MWCNTs-COOH and accounted for 14% of the bacterial community (*Fig. 4*). In addition, *Methanosarcina* was large enriched in the presence of MWCNTs-COOH. Previous studies also showed that the abundance of *Geobacter* species as well as the conductive materials, simultaneously enhance the growth of *Geobacter* and the  $\text{CH}_4$  production in the methanogenic soils (*Kato, Hashimoto & Watanabe, 2012; Li et al., 2015; Rotaru et al., 2015*). Owing to the high electrical conductivity of MWCNTs-COOH, it seems that MWCNTs-COOH have a similar function with  $\text{Fe}_3\text{O}_4$  to facilitate DIET in syntrophic methanogenesis from propionate. However, in this study, we did not have sufficient evidence to support the occurrence of DIET in the syntrophic consortia from propionate oxidation. In particular, the study from *Salvador et al. (2017)* suggested that CNTs significantly accelerated the  $\text{CH}_4$  production directly by pure methanogens and that the direct effect was independent of possible mechanisms, such as DIET. Convincing mechanisms for the simulation of  $\text{CH}_4$  production from propionate oxidation are still unknown. Elucidation of the mechanisms that enhance  $\text{CH}_4$  production will require much more extensive investigation with novel approaches in future work.

Recent studies showed that CNTs could also stimulate  $\text{CH}_4$  production in lake sediments with butyrate oxidation, anaerobic reactors with beet sugar digestion and pure cultures of methanogens (*Ambuchi et al., 2017; Salvador et al., 2017; Zhang & Lu, 2016*). However, the effect of MWCNTs-COOH on the syntrophic consortia from propionate oxidation in paddy soil enrichment was never reported. Our study verified that the MWCNTs-COOH could change the relative abundance of the dominant bacterial and archaeal genera in paddy soil enrichment (*Fig. 4*). *Smithella* utilize propionate in a nonrandomizing pathway in which propionate is first dismutated to acetate and butyrate before being degraded via  $\beta$ -oxidation, while *Syntrophomonas* are known butyrate degraders (*Dolfing, 2013; Gan et al., 2012; Lueders, Pommerenke & Friedrich, 2004*). There were increases in the relative abundances of the bacterial genera such as *Geobacter*, *Smithella*, *Syntrophomonas* and the archaeal genera such as *Methanosarcina* in the MWCNTs-COOH treatment. However, there were no significant differences in the bacterial and archaeal community compositions



during the enrichment. Recent studies also showed that microbe community structure significantly shifted after CNTs addition (*Ambuchi et al., 2017; Shrestha et al., 2013; Zhang & Lu, 2016*). For example, the bacterial genera such as *Rhodococcus*, *Cellulomonas* and *Nocardioides* were increased after the addition of 1 g/kg MWCNTs in sandy loam soil (*Shrestha et al., 2013*). In addition, the fungal genera *Pseudeurotium* and *Penicillium* (important in the soil carbon and phosphorus biogeochemical cycling) were decreased after the addition of 0.5 g/kg CNTs into a grass soil (*Rodrigues, Jaisi & Elimelech, 2013*).

By 2011, the worldwide CNTs production had jumped to about 4.6 kilotons per year (*De Volder et al., 2013*). As they are adopted for increasing use in consumer products, there is a potential for CNTs to enter the environment through both accidental discharge and intentional application. Potential CNTs release mechanisms during the CNTs/polymer lifecycle include biodegradation, washing, diffusion, matrix degradation and incineration (*Petersen et al., 2011*). While many previous studies have been focused on the toxicity of these materials to microorganisms and human health, our study prompts further investigation to evaluate the various consequences of nanomaterial release into anoxic natural environments.

## CONCLUSIONS

The supplementation of MWCNTs-COOH displayed a substantial stimulatory effect on anaerobic syntrophic CH<sub>4</sub> production in paddy soil enrichment. MWCNTs-COOH exerted positive, rather than cytotoxic, effects on the microbes involved in syntrophic methanogenesis from propionate degradation and affected the bacterial and archaeal community structure in the test concentrations.

## ACKNOWLEDGEMENTS

We thank Prof. Yahai Lu in the Peking University for helping advice and support.

## ADDITIONAL INFORMATION AND DECLARATIONS

### Funding

This work was supported by National Key R&D Program of China (Nos. 2016YFD0200306 and 2016YFA0601000) and the National Natural Science Foundation of China (41671294; 41701275). The funders had no role in study design, data collection and analysis, decision to publish, or preparation of the manuscript.

### Grant Disclosures

The following grant information was disclosed by the authors:

National Key R&D Program of China: 2016YFD0200306, 2016YFA0601000.

National Natural Science Foundation of China: 41671294, 41701275.

### Competing Interests

The authors declare there are no competing interests.

### Author Contributions

- Jianchao Zhang conceived and designed the experiments, performed the experiments, analyzed the data, contributed reagents/materials/analysis tools, wrote the paper, prepared figures and/or tables.
- Xingxuan Xia performed the experiments, prepared figures and/or tables.
- Siliang Li contributed reagents/materials/analysis tools.
- Wei Ran wrote the paper.

### Data Availability

The following information was supplied regarding data availability:

NCBI: [SRP108450](#).

### Supplemental Information

Supplemental information for this article can be found online at <http://dx.doi.org/10.7717/peerj.4267#supplemental-information>.

## REFERENCES

- Ambuchi JJ, Zhang Z, Shan L, Liang D, Zhang P, Feng Y. 2017. Response of anaerobic granular sludge to iron oxide nanoparticles and multi-wall carbon nanotubes during beet sugar industrial wastewater treatment. *Water Research* 117:87–94 DOI 10.1016/j.watres.2017.03.050.
- Caporaso JG, Kuczynski J, Stombaugh J, Bittinger K, Bushman FD, Costello EK, Fierer N, Peña AG, Goodrich JK, Gordon JI, Huttley GA, Kelley ST, Knights D, Koenig JE, Ley RE, Lozupone CA, McDonald D, Muegge BD, Pirrung M, Reeder J, Sevinsky JR, Turnbaugh PJ, Walters WA, Widmann J, Yatsunencko T, Zaneveld J, Knight R. 2010. QIIME allows analysis of high-throughput community sequencing data. *Nature Methods* 7:335–336 DOI 10.1038/nmeth.f.303.
- Conrad R. 2009. The global methane cycle: recent advances in understanding the microbial processes involved. *Environmental Microbiology Reports* 1:285–292 DOI 10.1111/j.1758-2229.2009.00038.x.
- Das R, Abd Hamid SB, Ali ME, Ismail AF, Annuar MSM, Ramakrishna S. 2014. Multifunctional carbon nanotubes in water treatment: the present, past and future. *Desalination* 354:160–179 DOI 10.1016/j.desal.2014.09.032.
- De Volder MF, Tawfick SH, Baughman RH, Hart AJ. 2013. Carbon nanotubes: present and future commercial applications. *Science* 339:535–539 DOI 10.1126/science.1222453.
- Dolfing J. 2013. Syntrophic propionate oxidation via butyrate: a novel window of opportunity under methanogenic conditions. *Applied and Environmental Microbiology* 79:4515–4516 DOI 10.1128/AEM.00111-13.
- Du J, Wang S, You H, Zhao X. 2013. Understanding the toxicity of carbon nanotubes in the environment is crucial to the control of nanomaterials in producing and processing and the assessment of health risk for human: a review. *Environmental Toxicology and Pharmacology* 36:451–462 DOI 10.1016/j.etap.2013.05.007.



- Edgar RC. 2013.** UPARSE: highly accurate OTU sequences from microbial amplicon reads. *Nature Methods* **10**:996–998 DOI [10.1038/nmeth.2604](https://doi.org/10.1038/nmeth.2604).
- Farré M, Gajda-Schranz K, Kantiani L, Barceló D. 2009.** Ecotoxicity and analysis of nanomaterials in the aquatic environment. *Analytical and Bioanalytical Chemistry* **393**:81–95 DOI [10.1007/s00216-008-2458-1](https://doi.org/10.1007/s00216-008-2458-1).
- Gan Y, Qiu Q, Liu P, Rui J, Lu Y. 2012.** Syntrophic oxidation of propionate in rice field soil at 15 and 30 °C under methanogenic conditions. *Applied and Environmental Microbiology* **78**:4923–4932 DOI [10.1128/AEM.00688-12](https://doi.org/10.1128/AEM.00688-12).
- Gottschalk F, Sonderer T, Scholz RW, Nowack B. 2009.** Modeled environmental concentrations of engineered nanomaterials (TiO<sub>2</sub>, ZnO, Ag, CNT, Fullerenes) for different regions. *Environmental Science & Technology* **43**:9216–9222 DOI [10.1021/es9015553](https://doi.org/10.1021/es9015553).
- Greuter D, Loy A, Horn M, Rattei T. 2016.** probeBase—an online resource for rRNA-targeted oligonucleotide probes and primers: new features 2016. *Nucleic Acids Research* **44**:D586–D589 DOI [10.1093/nar/gkv1232](https://doi.org/10.1093/nar/gkv1232).
- Holmes DE, Shrestha PM, Walker DJF, Dang Y, Nevin KP, Woodard TL, Lovley DR. 2017.** Metatranscriptomic evidence for direct interspecies electron transfer between *Geobacter* and *Methanotrix* Species in methanogenic rice paddy soils. *Applied and Environmental Microbiology* **83**:e00223–00217 DOI [10.1128/AEM.00223-17](https://doi.org/10.1128/AEM.00223-17).
- Iijima S. 1991.** Helical microtubules of graphitic carbon. *Nature* **354**:56–58 DOI [10.1038/354056a0](https://doi.org/10.1038/354056a0).
- Kang S, Mauter MS, Elimelech M. 2008.** Physicochemical determinants of multiwalled carbon nanotube bacterial cytotoxicity. *Environmental Science & Technology* **42**:7528–7534 DOI [10.1021/es8010173](https://doi.org/10.1021/es8010173).
- Kang S, Pinault M, Pfefferle LD, Elimelech M. 2007.** Single-walled carbon nanotubes exhibit strong antimicrobial activity. *Langmuir* **23**:8670–8673 DOI [10.1021/la701067r](https://doi.org/10.1021/la701067r).
- Kato S, Hashimoto K, Watanabe K. 2012.** Methanogenesis facilitated by electric syntrophy via (semi) conductive iron-oxide minerals. *Environmental Microbiology* **14**:1646–1654 DOI [10.1111/j.1462-2920.2011.02611.x](https://doi.org/10.1111/j.1462-2920.2011.02611.x).
- Krumböck M, Conrad R. 1991.** Metabolism of position-labelled glucose in anoxic methanogenic paddy soil and lake sediment. *FEMS Microbiology Letters* **85**:247–256 DOI [10.1111/j.1574-6968.1991.tb04731.x](https://doi.org/10.1111/j.1574-6968.1991.tb04731.x).
- Li H, Chang J, Liu P, Fu L, Ding D, Lu Y. 2015.** Direct interspecies electron transfer accelerates syntrophic oxidation of butyrate in paddy soil enrichments. *Environmental Microbiology* **17**:1533–1547 DOI [10.1111/1462-2920.12576](https://doi.org/10.1111/1462-2920.12576).
- Liu F, Rotaru A-E, Shrestha PM, Malvankar NS, Nevin KP, Lovley DR. 2012.** Promoting direct interspecies electron transfer with activated carbon. *Energy & Environmental Science* **5**:8982–8989 DOI [10.1039/c2ee22459c](https://doi.org/10.1039/c2ee22459c).
- Liu F, Rotaru A-E, Shrestha PM, Malvankar NS, Nevin KP, Lovley DR. 2015.** Magnetite compensates for the lack of a pilin-associated c-type cytochrome in extracellular electron exchange. *Environmental Microbiology* **17**:648–655 DOI [10.1111/1462-2920.12485](https://doi.org/10.1111/1462-2920.12485).

- Lü Z, Lu Y. 2012. *Methanocella conradii* sp. nov., a thermophilic, obligate hydrogenotrophic methanogen, isolated from Chinese rice field soil. *PLOS ONE* 7:e35279 DOI 10.1371/journal.pone.0035279.
- Lueders T, Pommerenke B, Friedrich MW. 2004. Stable-isotope probing of microorganisms thriving at thermodynamic limits: syntrophic propionate oxidation in flooded soil. *Applied and Environmental Microbiology* 70:5778–5786 DOI 10.1128/AEM.70.10.5778-5786.2004.
- Mach V, Blaser MB, Claus P, Chaudhary PP, Rulík M. 2015. Methane production potentials, pathways, and communities of methanogens in vertical sediment profiles of river Sitka. *Frontiers in Microbiology* 6:506 DOI 10.3389/fmicb.2015.00506.
- Mahadevan R, Palsson BØ, Lovley DR. 2011. *In situ* to in silico and back: elucidating the physiology and ecology of *Geobacter* spp. using genome-scale modelling. *Nature Reviews Microbiology* 9:39–50 DOI 10.1038/nrmicro2456.
- Morita M, Malvankar NS, Franks AE, Summers ZM, Giloteaux L, Rotaru AE, Rotaru C, Lovley DR. 2011. Potential for direct interspecies electron transfer in methanogenic wastewater digester aggregates. *MBio* 2:e00159–00111 DOI 10.1128/mBio.00159-11.
- Moter A, Göbel UB. 2000. Fluorescence *in situ* hybridization (FISH) for direct visualization of microorganisms. *Journal of Microbiological Methods* 41:85–112 DOI 10.1016/S0167-7012(00)00152-4.
- Nouara A, Wu Q, Li Y, Tang M, Wang H, Zhao Y, Wang D. 2013. Carboxylic acid functionalization prevents the translocation of multi-walled carbon nanotubes at predicted environmentally relevant concentrations into targeted organs of nematode *Caenorhabditis elegans*. *Nanoscale* 5:6088–6096 DOI 10.1039/c3nr00847a.
- Nowack B, David RM, Fissan H, Morris H, Shatkin JA, Stintz M, Zepp R, Brouwer D. 2013. Potential release scenarios for carbon nanotubes used in composites. *Environment International* 59:1–11 DOI 10.1016/j.envint.2013.04.003.
- Peng J, Lü Z, Rui J, Lu Y. 2008. Dynamics of the methanogenic archaeal community during plant residue decomposition in an anoxic rice field soil. *Applied and Environmental Microbiology* 74:2894–2901 DOI 10.1128/AEM.00070-08.
- Petersen EJ, Zhang L, Mattison NT, O'Carroll DM, Whelton AJ, Uddin N, Nguyen T, Huang Q, Henry TB, Holbrook RD, Chen KL. 2011. Potential release pathways, environmental fate, and ecological risks of carbon nanotubes. *Environmental Science & Technology* 45:9837–9856 DOI 10.1021/es201579y.
- Qu X, Alvarez PJ, Li Q. 2013. Photochemical transformation of carboxylated multiwalled carbon nanotubes: role of reactive oxygen species. *Environmental Science & Technology* 47:14080–14088 DOI 10.1021/es4033056.
- Richter K, Schicklberger M, Gescher J. 2012. Dissimilatory reduction of extracellular electron acceptors in anaerobic respiration. *Applied and Environmental Microbiology* 78:913–921 DOI 10.1128/AEM.06803-11.
- Rodrigues DF, Jaisi DP, Elimelech M. 2013. Toxicity of functionalized single-walled carbon nanotubes on soil microbial communities: implications for nutrient cycling in soil. *Environmental Science & Technology* 47:625–633 DOI 10.1021/es304002q.

- Rotaru A-E, Shrestha PM, Liu F, Markovaite B, Chen S, Nevin KP, Lovley DR. 2014a.** Direct Interspecies electron transfer between *Geobacter metallireducens* and *Methanosarcina barkeri*. *Applied and Environmental Microbiology* **80**:4599–4605 DOI [10.1128/AEM.00895-14](https://doi.org/10.1128/AEM.00895-14).
- Rotaru A-E, Shrestha PM, Liu F, Shrestha M, Shrestha D, Embree M, Zengler K, Wardman C, Nevin KP, Lovley DR. 2014b.** A new model for electron flow during anaerobic digestion: direct interspecies electron transfer to *Methanosaeta* for the reduction of carbon dioxide to methane. *Energy & Environmental Science* **7**:408–415 DOI [10.1039/C3EE42189A](https://doi.org/10.1039/C3EE42189A).
- Rotaru A-E, Woodard TL, Nevin KP, Lovley DR. 2015.** Link between capacity for current production and syntrophic growth in *Geobacter* species. *Frontiers in Microbiology* **6**:744 DOI [10.3389/fmicb.2015.00744](https://doi.org/10.3389/fmicb.2015.00744).
- Salvador AF, Martins G, Melle-Franco M, Serpa R, Stams AJM, Cavaleiro AJ, Pereira MA, Alves MM. 2017.** Carbon nanotubes accelerate methane production in pure cultures of methanogens and in a syntrophic coculture. *Environmental Microbiology* **19**:2727–2739 DOI [10.1111/1462-2920.13774](https://doi.org/10.1111/1462-2920.13774).
- Shrestha B, Acosta-Martinez V, Cox SB, Green MJ, Li S, Cañas-Carrell JE. 2013.** An evaluation of the impact of multiwalled carbon nanotubes on soil microbial community structure and functioning. *Journal of Hazardous Materials* **261**:188–197 DOI [10.1016/j.jhazmat.2013.07.031](https://doi.org/10.1016/j.jhazmat.2013.07.031).
- Shrestha PM, Rotaru A-E. 2014.** Plugging in or going wireless: strategies for interspecies electron transfer. *Frontiers in Microbiology* **5**:237 DOI [10.3389/fmicb.2014.00237](https://doi.org/10.3389/fmicb.2014.00237).
- Stams AJM, Plugge CM. 2009.** Electron transfer in syntrophic communities of anaerobic bacteria and archaea. *Nature Reviews Microbiology* **7**:568–577 DOI [10.1038/nrmicro2166](https://doi.org/10.1038/nrmicro2166).
- Vardharajula S, Ali SZ, Tiwari PM, Eroğlu E, Vig K, Dennis VA, Singh SR. 2012.** Functionalized carbon nanotubes: biomedical applications. *International Journal of Nanomedicine* **7**:5361–5374 DOI [10.2147/IJN.S35832](https://doi.org/10.2147/IJN.S35832).
- Viggi CC, Rossetti S, Fazi S, Paiano P, Majone M, Aulenta F. 2014.** Magnetite particles triggering a faster and more robust syntrophic pathway of methanogenic propionate degradation. *Environmental Science & Technology* **48**:7536–7543 DOI [10.1021/es5016789](https://doi.org/10.1021/es5016789).
- Wang Q, Garrity GM, Tiedje JM, Cole JR. 2007.** Naïve bayesian classifier for rapid assignment of rRNA sequences into the new bacterial taxonomy. *Applied and Environmental Microbiology* **73**:5261–5267 DOI [10.1128/AEM.00062-07](https://doi.org/10.1128/AEM.00062-07).
- Wang C, Liu H, Chen J, Tian Y, Shi J, Li D, Guo C, Ma Q. 2014.** Carboxylated multi-walled carbon nanotubes aggravated biochemical and subcellular damages in leaves of broad bean (*Vicia faba* L.) seedlings under combined stress of lead and cadmium. *Journal of Hazardous Materials* **274**:404–412 DOI [10.1016/j.jhazmat.2014.04.036](https://doi.org/10.1016/j.jhazmat.2014.04.036).
- Yadav T, Mungray AA, Mungray AK. 2016.** Effect of multiwalled carbon nanotubes on UASB microbial consortium. *Environmental Science and Pollution Research* **23**:4063–4072 DOI [10.1007/s11356-015-4385-y](https://doi.org/10.1007/s11356-015-4385-y).

**Zhang J, Lu Y. 2016.** Conductive Fe<sub>3</sub>O<sub>4</sub> nanoparticles accelerate syntrophic methane production from butyrate oxidation in two different lake sediments. *Frontiers in Microbiology* 7:1316 DOI [10.3389/fmicb.2016.01316](https://doi.org/10.3389/fmicb.2016.01316).

**Zhao X, Liu R. 2012.** Recent progress and perspectives on the toxicity of carbon nanotubes at organism, organ, cell, and biomacromolecule levels. *Environment International* 40:244–255 DOI [10.1016/j.envint.2011.12.003](https://doi.org/10.1016/j.envint.2011.12.003).